N63-18470

NASA TN D-1975

NASA TN D-1975

TECHNICAL NOTE

D-1975

HEAT TRANSFER TO BLUNT CONICAL BODIES HAVING

CAVITIES TO PROMOTE SEPARATION

By Frank J. Centolanzi

Ames Research Center
Moffett Field, Calif.

NATIONAL AERONAUTICS AND SPACE ADMINISTRATION

WASHINGTON July 1963

NATIONAL AERONAUTICS AND SPACE ADMINISTRATION

TECHNICAL NOTE D-1975

HEAT TRANSFER TO BLUNT CONICAL BODIES HAVING CAVITIES TO PROMOTE SEPARATION

By Frank J. Centolanzi

SUMMARY

A wind-tunnel investigation of the heat transfer to conical configurations with cavities to promote boundary-layer separation was conducted at Mach numbers ranging from 3.98 to 5.79 and Reynolds numbers of 0.12 to 0.19 million based on model diameter. Both sharp and blunt cones were tested.

The results show that the presence of a cavity changes the distribution of heat transfer considerably. From the standpoint of total heat transfer there is an adverse effect of separating the boundary layer because heat transfer in the reattachment region is high and affects a considerable fraction of the total surface area.

Wall cooling had a strong influence on the flow over some of the models with cavities. On some models, extreme wall cooling caused the transition point to move upstream. In one case, extreme wall cooling caused completely attached flow over a model which had a separated laminar boundary layer under adiabatic conditions.

Under certain test conditions, the flow over a model with a cavity was found to pulsate. With pulsating flow the distribution of heat transfer is similar to that observed for steady separated flow.

INTRODUCTION

Theoretical and experimental studies have indicated that the aerodynamic heating of vehicles may be reduced in regions where the boundary layer is separated. In reference 1 Chapman presented a theoretical analysis of heat transfer which indicated that separation of a laminar boundary layer reduces the average heat transfer 44 percent. On the other hand, the analysis indicated that separation of a turbulent boundary layer can either increase or decrease the heat transfer, depending on the local Mach number. Experimental data on heat transfer in cylindrical and two-dimensional separated flows (ref. 2) are in agreement with the theory of reference 1 for laminar but not for turbulent flows. Measurements on a 10° half-angle cone having a cavity in order to separate the boundary layer (ref. 3) show that the total heat transfer in the cavity was reduced as predicted by the theory of reference 1. The heat transfer just downstream of the cavity, however, was increased considerably. Because of this, the total heat transfer to the cone was essentially unchanged by a cavity.

For blunt aerodynamic configurations the highest heating rates occur on the frontal surfaces. The results of the previous theoretical and experimental investigations leave unanswered the question of whether separating the flow would reduce the heating on blunt bodies. The purpose of the present tests was to explore this possibility for blunt reentry bodies having cavities to separate the boundary layer.

SYMBOLS

b skin thickness, ft

c_p specific heat, $\frac{Btu}{lb\text{-}^{\circ}R}$

M Mach number

q local heat-transfer rate, $\frac{Btu}{sec\text{-}ft^2}$

Q total heat transfer, $\frac{Btu}{sec}$

r local radius, measured from axis of symmetry, ft

Re Reynolds number

s arc length, measured along unmodified cone length, ft

s_m value of s, measured at maximum radius of model, ft

T temperature, $^{\circ}R$

ρ density, lb/ft^3

τ time, sec

Subscripts

t total

w wall

∞ free-stream conditions

APPARATUS

The tests were conducted in the Ames 1- by 3-Foot Supersonic Wind Tunnel No. 1.

The details of the heat-transfer models are shown in figure 1. The models were constructed of electroformed nickel. The nickel was electrodeposited on an aluminum mandrel to a thickness of about 0.030 inch and then machined to a nominal thickness of 0.010 inch. The aluminum mandrel was dissolved in a solution of sodium hydroxide leaving a hollow, thin-walled model. The thickness distributions of the models were measured to determine the heat storage capacity of the skin.

The general arrangement for cooling the models is shown in the photographs of figure 2. The cylindrical portion of the cooling apparatus slid forward to cover the models while they were being cooled to the desired temperatures. This arrangement insured that the model surfaces were free of frost and essentially isothermal at the start of the run. The spray nozzle and cylinder were activated by pneumatic air cylinders and were completely retracted in about 80 milliseconds.

The models were instrumented with copper-constantan thermocouples at the locations indicated in table I. The output signal from the thermocouples was amplified and differentiated electronically. The variations of T and $dT/d\tau$ with time were recorded on multichannel oscillographs.

The details of the flow over the models were recorded on film by means of the spark shadowgraph technique. The spark source, whose exposure time was about 0.2 microsecond, was triggered when the cooling mechanism was fully retracted.

TESTS AND PROCEDURE

The heat-transfer tests were conducted at Mach numbers ranging from 3.98 to 5.79. Most of the configurations were tested at the minimum Reynolds number available at each Mach number in an attempt to achieve fully laminar flow over the models. The Reynolds numbers ranged from 0.12 to 0.19 million based on model diameter.

The local heat transfer to the models was determined by the transient technique. The models were cooled with liquid nitrogen to their desired temperature. The cooling apparatus was then retracted and the variation of T and $dT/d\tau$ with time was recorded. The following equation was used to reduce the data

$$q = \rho b c_p (dT/d\tau)$$

In all cases the initial slope of the time-temperature curve was used to minimize the effects of conduction of heat along the skin.

RESULTS AND DISCUSSION

The primary objective of the investigation, as mentioned previously, was to determine the effect of separating the boundary layer on the heat transfer to conical bodies of revolution. Since the occurrence of separation was markedly affected by wall cooling, this effect will be discussed before the heat-transfer results. The effect of wall cooling on two of the models (1C and 1D) is shown in figure 3. At adiabatic conditions, the flow over both models is separated and laminar. Extreme cooling of the blunt-nosed model (1D) caused boundary-layer transition ahead of the reattachment point, whereas, on the sharp-nosed model (1C) the boundary layer became fully attached to the body. The latter effect was corroborated in tests of a model with the same forebody in an Ames free-flight range. Both these effects of wall cooling were also observed in reference 2 for cylindrical separated boundary layers.

Heat-Transfer Results

The local heating rates for each conical model with and without concavity are compared in figures 4 through 7. Data are presented for three wall temperatures, 0°, -150°, and -300° F. Spark shadowgraphs of the flow over the concave models are shown for each test condition.

For the pointed cone, without concavity, model 1A, the heat-transfer rates are also compared in figure 4 with those predicted by the theory of reference 4. In general, the theory is in fair agreement with experiment.

For the pointed cone with concavity, model 1C, extreme wall cooling ($T_w/T_t = 0.25$) causes the boundary layer to remain attached to the body. The distribution of heat transfer for this case (fig. 4) seems to follow that expected for attached flow over such a shape. The heat transfer in the forward portion of the cavity is about as low with attached flow ($T_w/T_t = 0.25$) as it is with separated flow ($T_w/T_t = 0.72$). For moderate cooling where the boundary layer is separated and laminar, the heat-transfer rates in the rearward half of the separated region are as much as 6 to 7 times higher than those for the cone without a cavity.

The heat-transfer rates to model 1D and model 1B are compared in figure 5. In general, the heat-transfer rates in the first 75 percent of the separated region of model 1D are considerably less than those for model 1B; whereas, the heat-transfer rates in the reattachment zone are about 5 to 6 times higher than those for model 1B.

An example of heat transfer in a separated region where the boundary layer is transitional is shown in figure 6. On model 2B with moderate wall cooling ($T_w/T_t = 0.76$) transition occurs at about $s/s_m = 0.7$; whereas, with extreme wall cooling ($T_w/T_t = 0.26$) transition moves upstream to about $s/s_m = 0.5$. The upstream movement of the transition point broadens the region in which the heat-transfer rates are high.

The results of measurements on models with high drag are shown in figure 7. It is not clear from examination of the shadowgraph pictures to what extent the flow over model 3B is separated. There appears to be little, if any, effect of wall cooling on the observed heat-transfer distribution.

Under certain conditions the flow over a concave model developed high-frequency pulsations. The results of heat-transfer measurements on a pulsating-flow model, 2C, are compared with those on an attached-flow model, 2A, in figure 8. Since the frequency of oscillation was rather high (of the order of thousands of cycles per second), the instrumentation recorded only temporal mean heating rates. The shadowgraph pictures show only one phase of the oscillation since they are single exposures. In general, the heat transfer with pulsating flow resembles that with steady separated flow.

The ratio of the total heat transfer in the cavity of model 1C to the equivalent attached flow portion of model 1A is compared with the theoretical predictions of reference 1 in figure 9.

The total heat transfer was determined by graphical integration of the equation (see sketch (a))

$$Q = 2\pi \int_a^b qr\, ds'$$

where q represents the local heat-transfer distributions presented in figure 4.

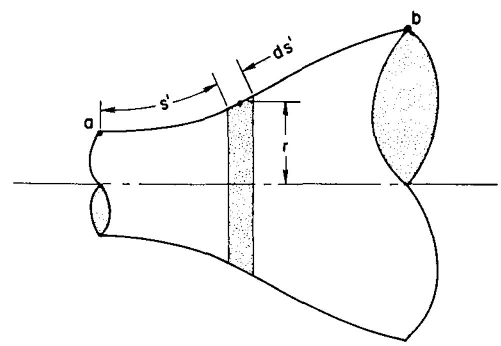

Sketch (a)

The results show that for moderate cooling ($T_w/T_t = 0.72$), the flow on the cone with the cavity is separated and fully laminar and the ratio of total heat transfer is about 1.7 times that for the cone without the cavity; whereas, for extreme cooling ($T_w/T_t = 0.25$), the flow is attached and the ratio is nearly equal to unity. From the standpoint of total heat transfer, experiment shows a very adverse effect of separating the boundary layer, in contrast to the theoretical prediction of a very favorable effect. The large reduction of heat transfer in the forward portion of the separated region is offset by the increased heat transfer in and downstream of the reattachment region. The maximum heat-transfer rates occur in a region which contains a large percentage of the total surface area. Probably the main reason for lack of agreement between the results of this investigation and the theory of reference 1 is that because of the geometry of the model in the reattachment region, the separated flow does not completely span the cavity. In order to make a fair comparison between these data and theory, for example, the limits of integration for determining the total heat transfer should extend only over the area that is truly separated. The fact still remains that, from the standpoint of total heat transfer for the cone model of figure 9, there is no over-all benefit of separating the boundary layer. Examination of the local heat transfer to the other models also indicates that no over-all benefit is derived from separating the boundary layer.

CONCLUSIONS

A wind-tunnel investigation was conducted to determine the effectiveness of boundary-layer separation in reducing the heat transfer to cones. The resulting data support the following conclusions:

1. If the shape of a cone is altered to form a cavity over which a laminar-separated boundary-layer flows, the distribution of heat transfer is changed considerably. In the forward portion of the cavity the heat transfer decreases; whereas, in the rearward portion the heat transfer increases in the reattachment region to a maximum which is several times that for attached flow.

2. From the standpoint of total heat transfer, there was an adverse effect of separating the boundary layer on the models tested. The large reduction of heat transfer in the forward portion of the separated region was offset by the increased heat-transfer rates over a much greater area in the vicinity of the reattachment region.

3. Wall cooling has a strong influence on the flow over some of the models with cavities. On some models, extreme wall cooling caused the transition point to move upstream. In one case, extreme wall cooling caused the flow to be completely attached over a model which had a separated laminar boundary layer under adiabatic wall conditions.

4. Under certain conditions the flow over a model having a cavity tended to pulsate. Under these conditions the heat-transfer rates were similar to those for steady separated flow.

Ames Research Center
National Aeronautics and Space Administration
Moffett Field, Calif., May 8, 1963

REFERENCES

1. Chapman, Dean R.: A Theoretical Analysis of Heat Transfer in Regions of Separated Flow. NACA TN 3792, 1956.

2. Larson, Howard K.: Heat Transfer in Separated Flows. Jour. Aero/Space Sci., vol. 26, no. 11, Nov. 1959, pp. 731-738.

3. Bogdonoff, S. M., and Vas, I. E.: Some Experiments on Hypersonic Separated Flows. ARS Jour., vol. 32, no. 10, Oct. 1962, pp. 1564-1572.

4. Eckert, E. R. G.: Engineering Relations for Friction and Heat Transfer to Surfaces in High Velocity Flow. Jour. Aero. Sci., vol. 22, no. 8, Aug. 1955, pp. 585-587.

5. Fay, J. A., and Riddell, F. R.: Theory of Stagnation Point Heat Transfer in Dissociated Air. Jour. Aero. Sci., vol. 25, no. 2, Feb. 1958, pp. 73-85, 121.

Table I - Thermocouple locations, - s/s_m

	Model designation								
No.	1A	1B	1C	1D	2A	2B	2C	3A	3B
1	.089	0	.088	0	0	0	0	0	0
2	.180	.087	.202	.087	.091	.091	.091	.060	.060
3	.266	.186	.265	.135	.181	.139	.179	.155	.155
4	.351	.277	.346	.207	.273	.206	.273	.253	.251
5	.442	.382	.463	.308	.364	.297	.364	.349	.352
6	.528	.473	.563	.452	.454	.432	.454	.445	.445
7	.620	.572	.668	.600	.547	.568	.547	.543	.544
8	.705	.677	.786	.745	.640	.706	.635	.636	.632
9	.790	.768	.866	.843	.732	.802	.730	.728	.730
10	.882	.867	.927	.916	.825	.864	.822	.825	.829
11	.960	.965	.968	.964	.910	.910	.910	.919	.918
12	1.000	1.000	1.000	1.000	1.000	1.000	1.000	1.000	1.000

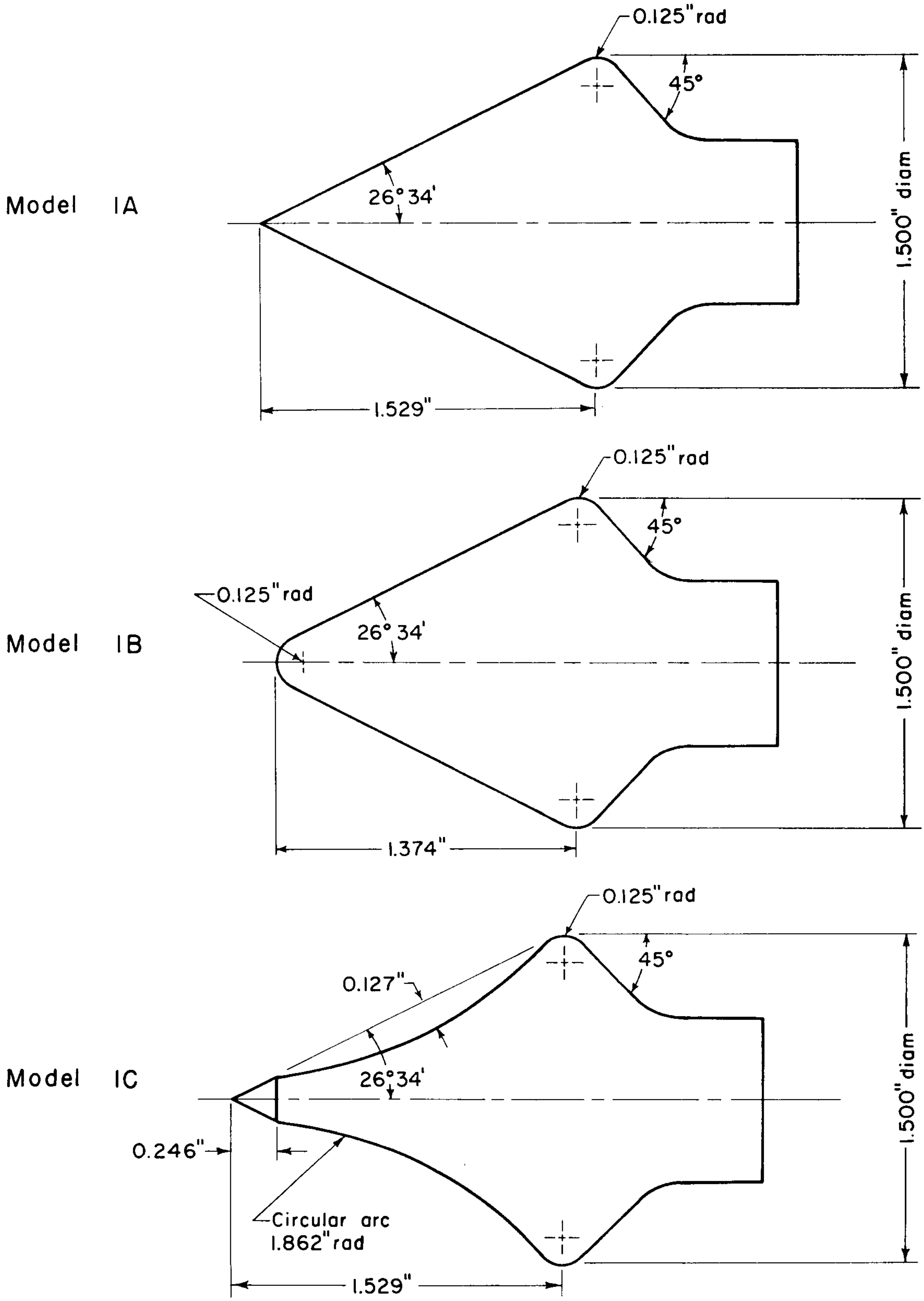

Figure 1.- Models.

Model 1D

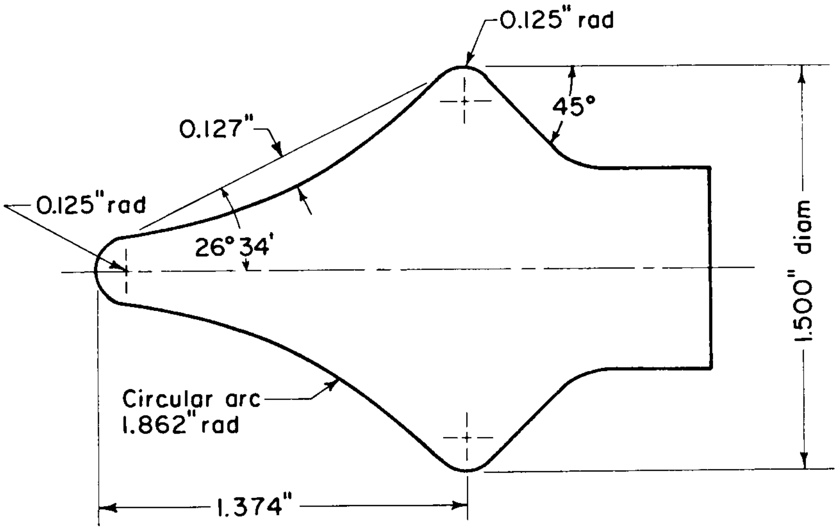

Model 2A

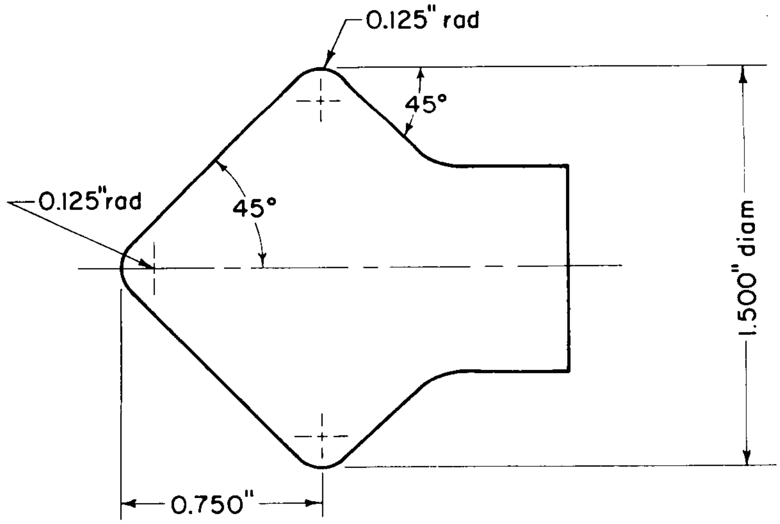

Model 2B

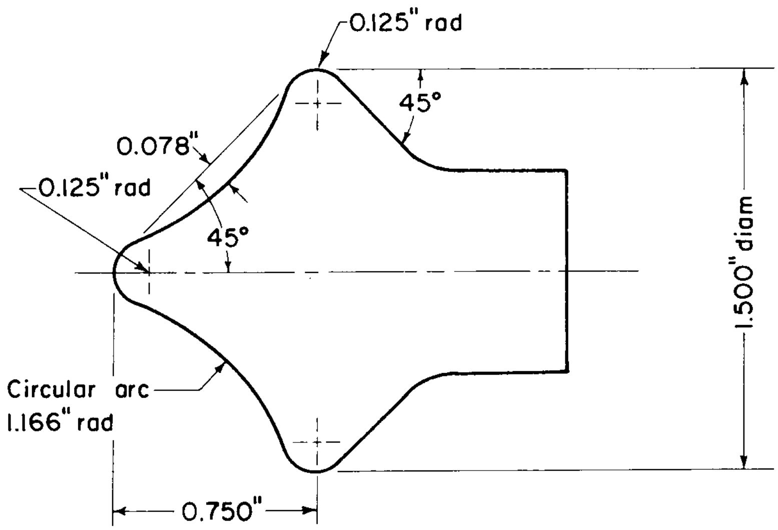

Figure 1.- Models - Continued.

Model 2C

Model 3A

Model 3B

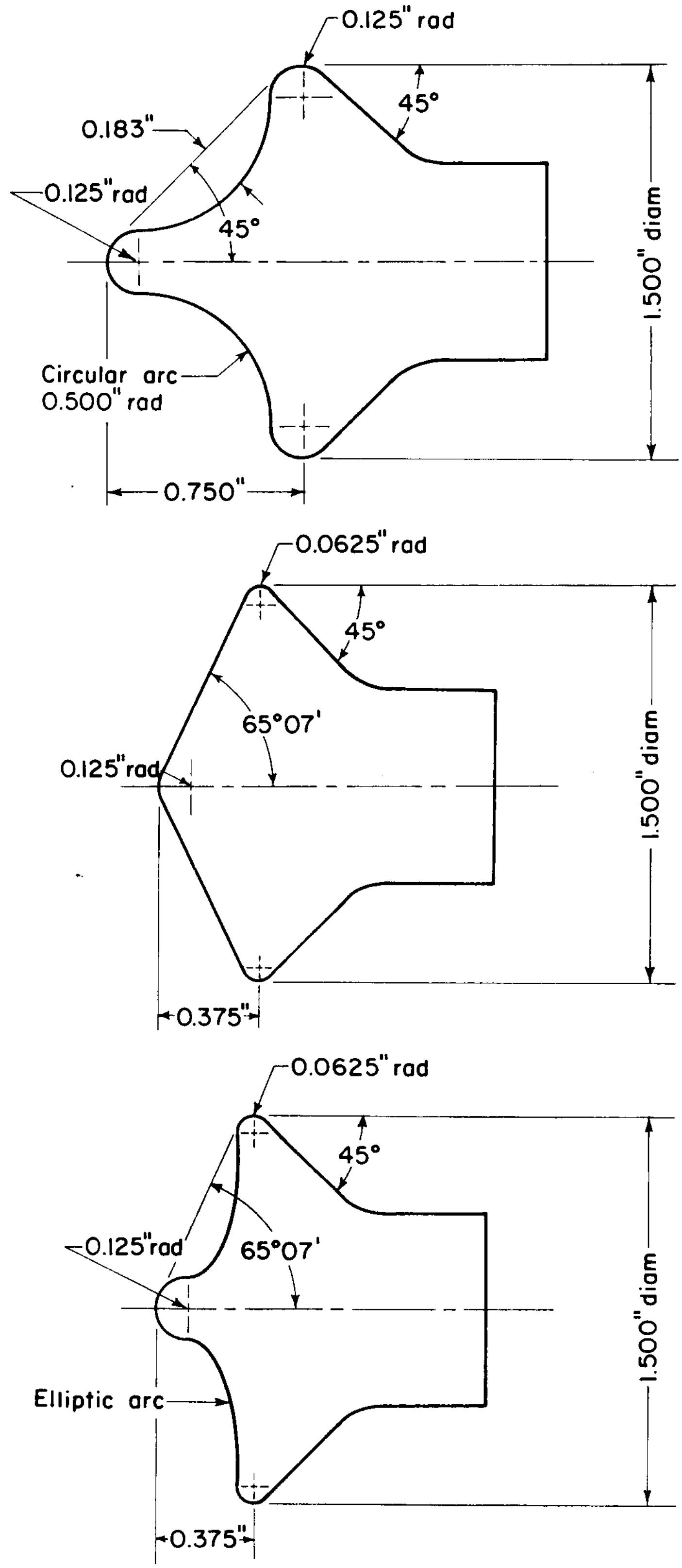

Figure 1.- Models - Concluded.

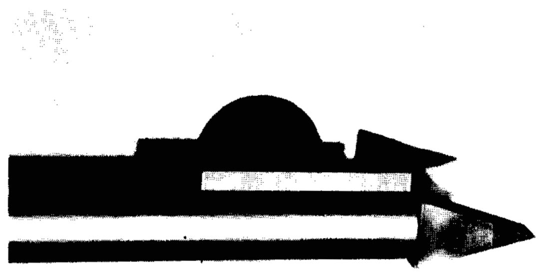

(a) Cooling mechanism closed

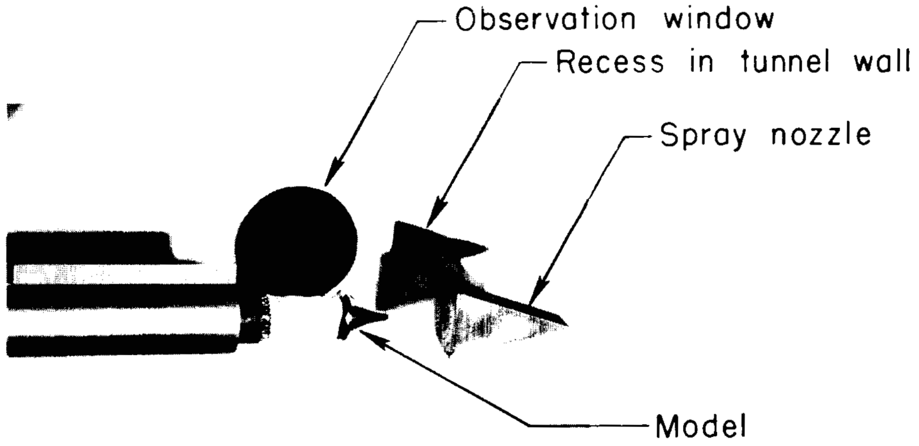

(b) Cylinder only retracted

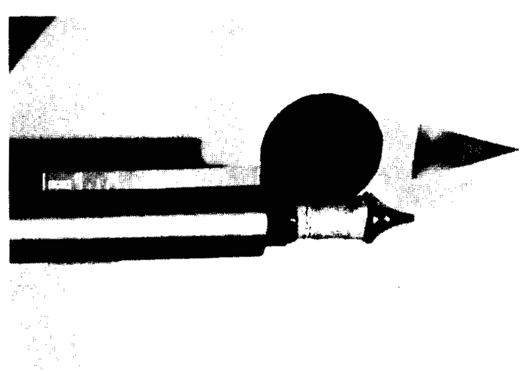

(c) Cooling mechanism fully retracted

Figure 2.- Tunnel installation.

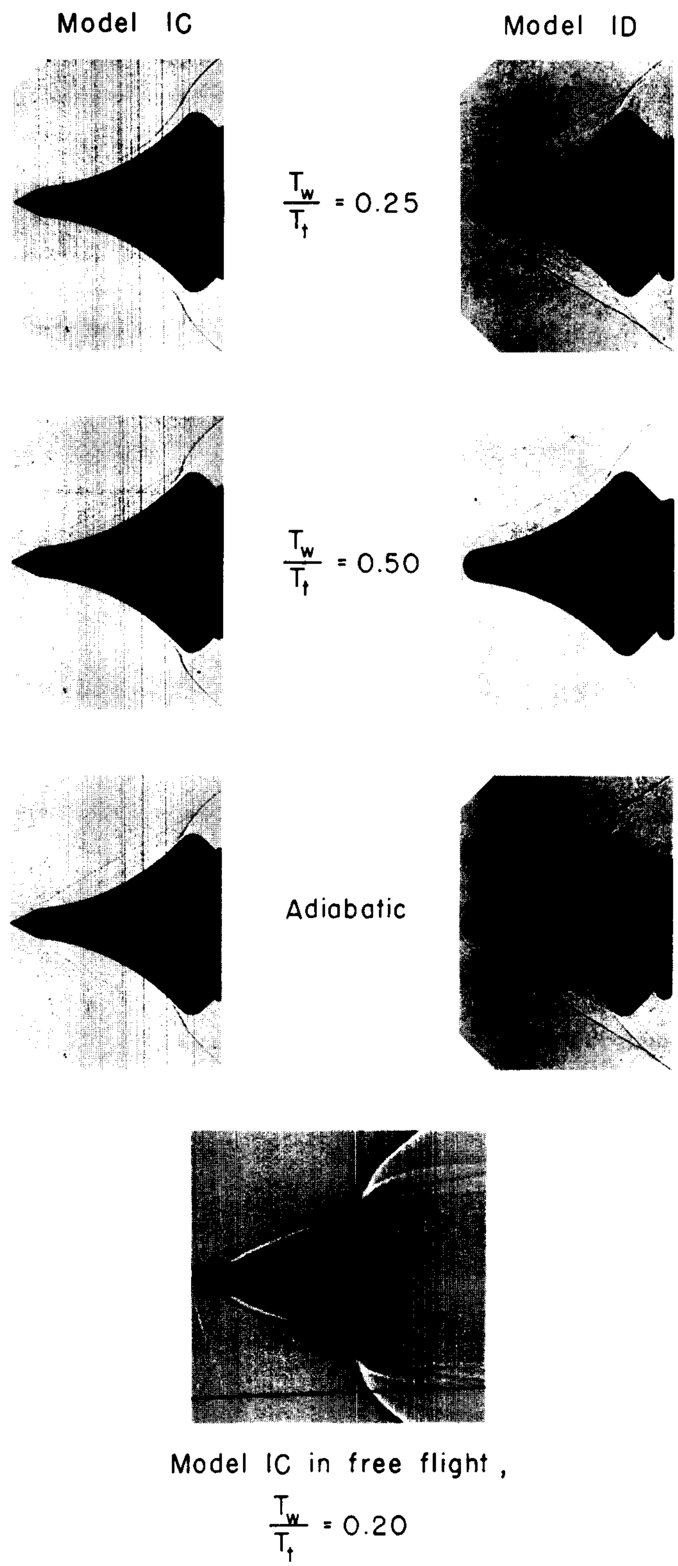

Figure 3.- Effect of wall cooling on separated laminar boundary layers; $M_\infty = 5.09$, $Re_\infty = 1.2 \times 10^6$, ft^{-1}.

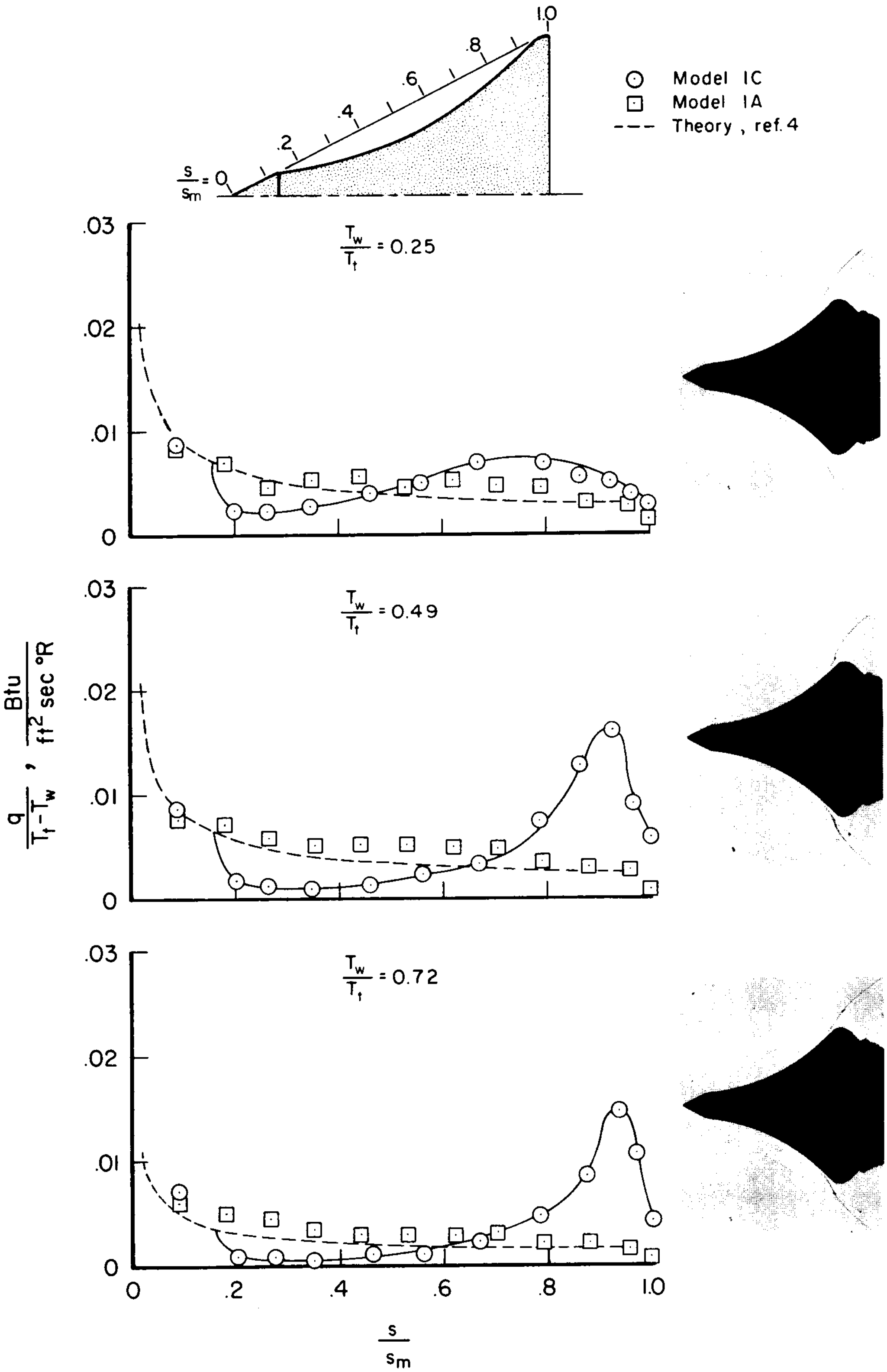

Figure 4.- Comparison of heat-transfer distribution between models 1A and 1C; $M_\infty = 5.09$, $Re_\infty = 1.2 \times 10^6$, ft^{-1}.

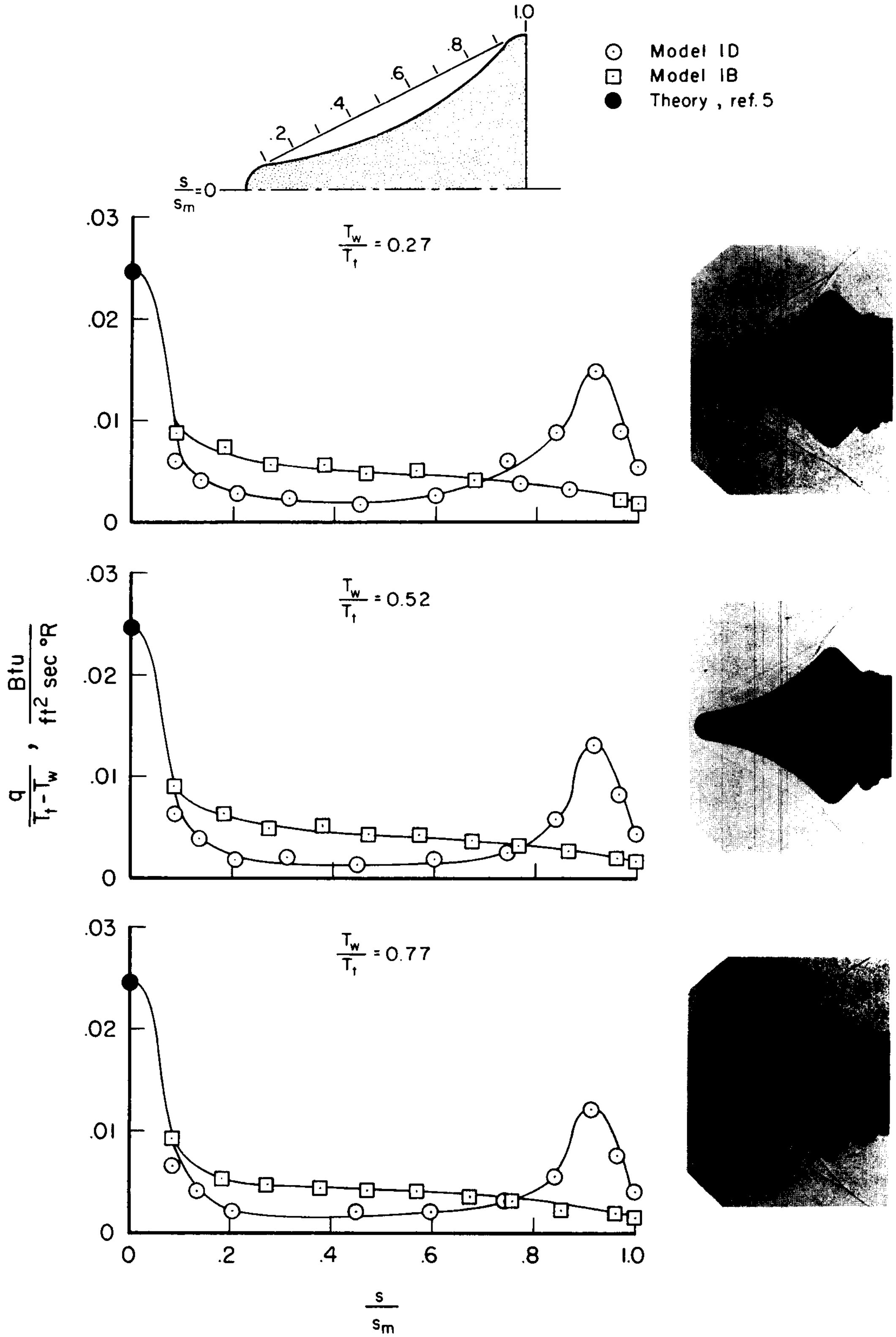

Figure 5.- Comparison of heat-transfer distribution between models 1B and 1D; $M_\infty = 5.09$, $Re_\infty = 1.2 \times 10^6$, ft^{-1}.

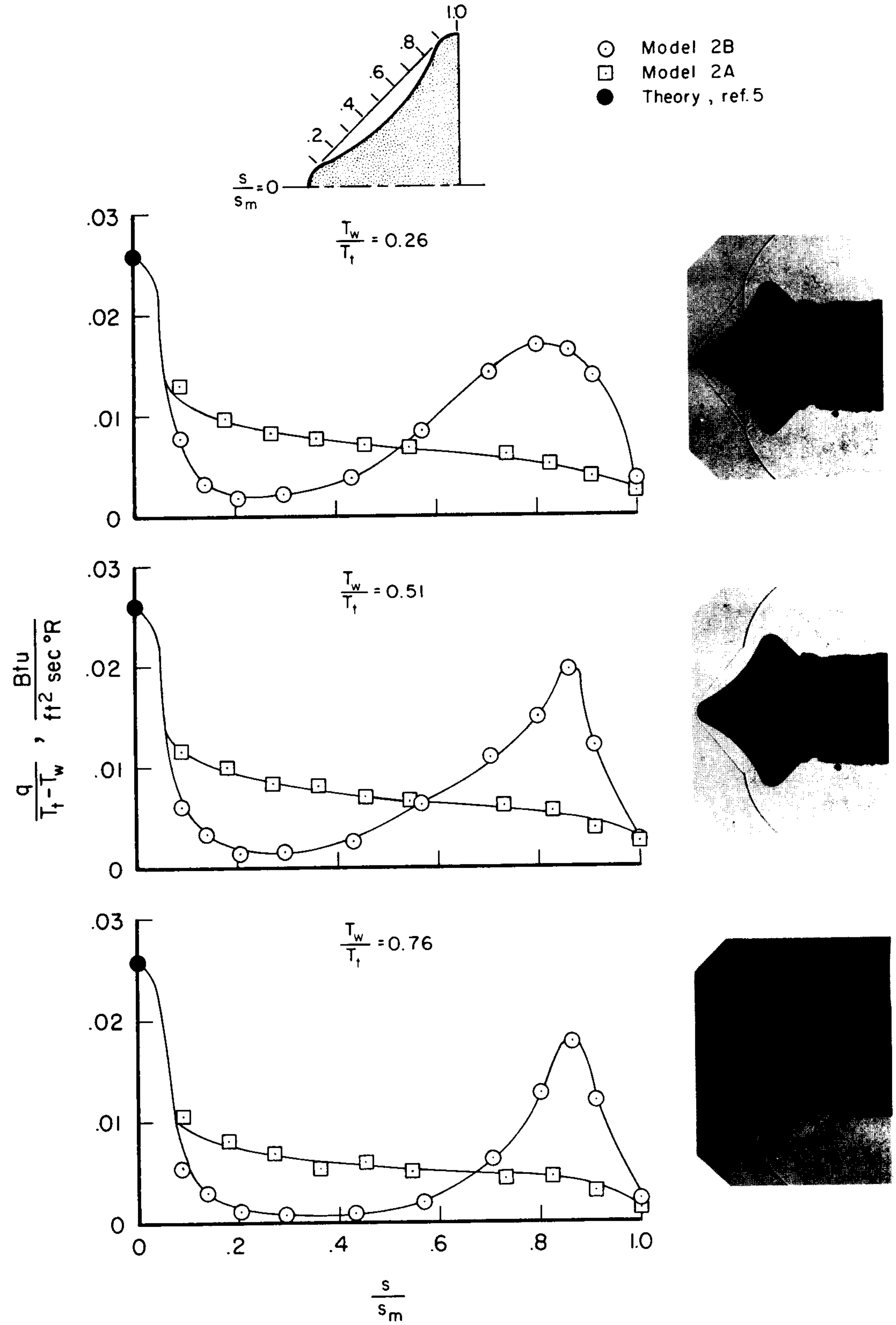

Figure 6.- Comparison of heat-transfer distribution between models 2A and 2B; $M_\infty = 5.79$, $Re_\infty = 1.5\times10^6$, ft^{-1}.

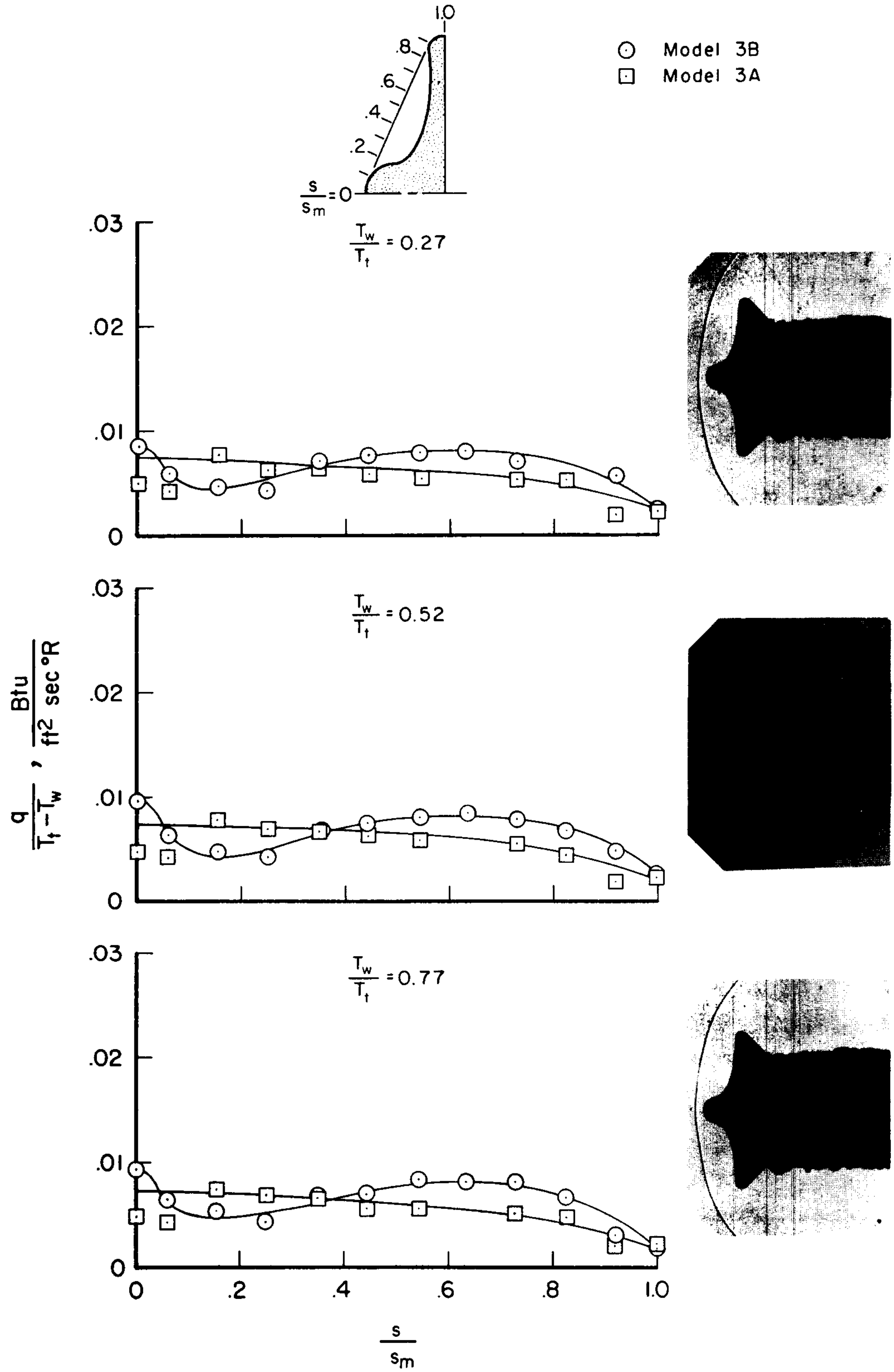

Figure 7.- Comparison of heat-transfer distribution between models 3A and 3B; $M_\infty = 5.09$, $Re_\infty = 1.2 \times 10^6$, ft^{-1}.

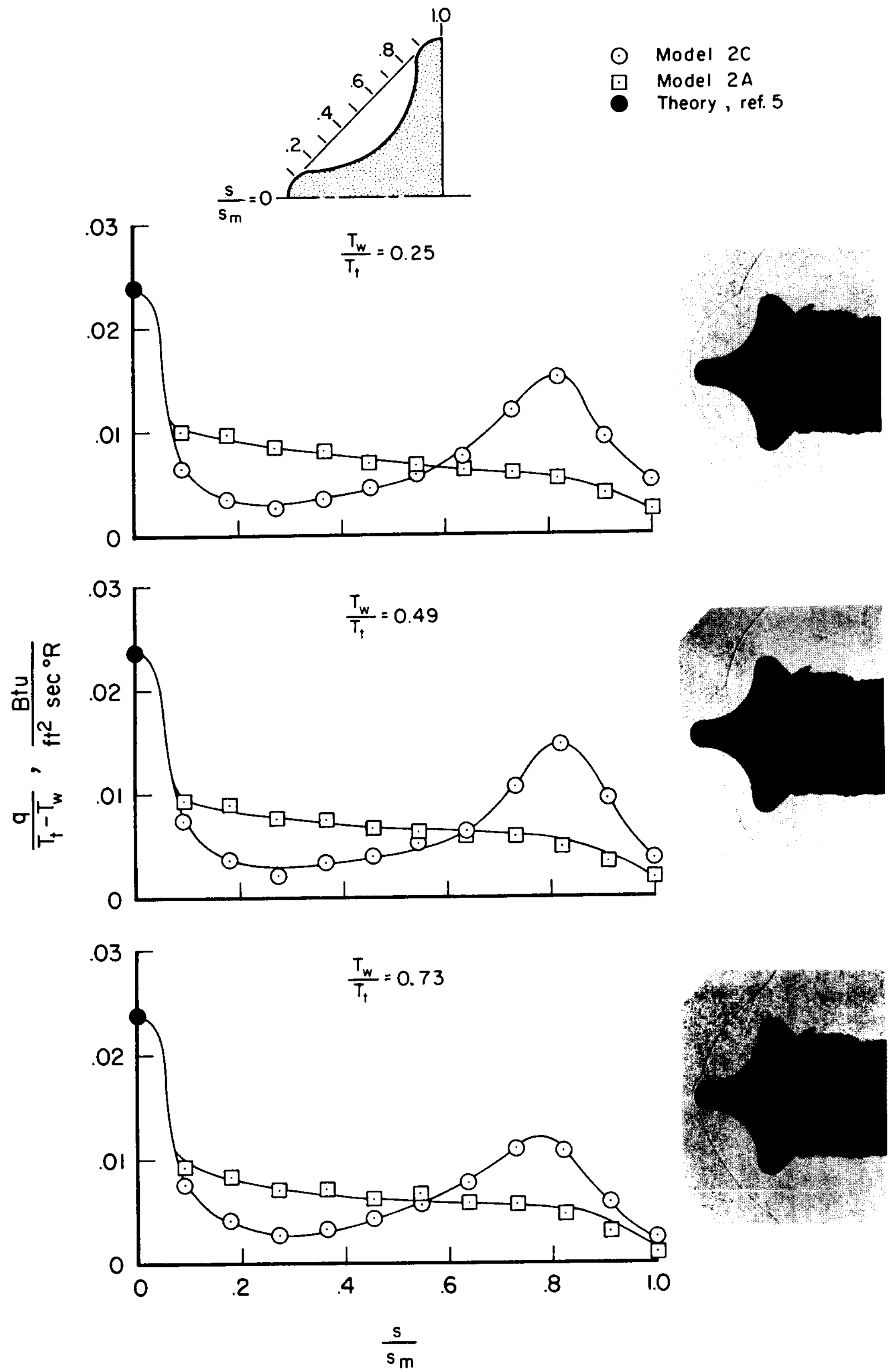

Figure 8.- Comparison of heat-transfer distribution between pulsating-flow model 2C and model 2A; $M_\infty = 3.98$, $Re_\infty = 10 \times 10^6$, ft^{-1}.

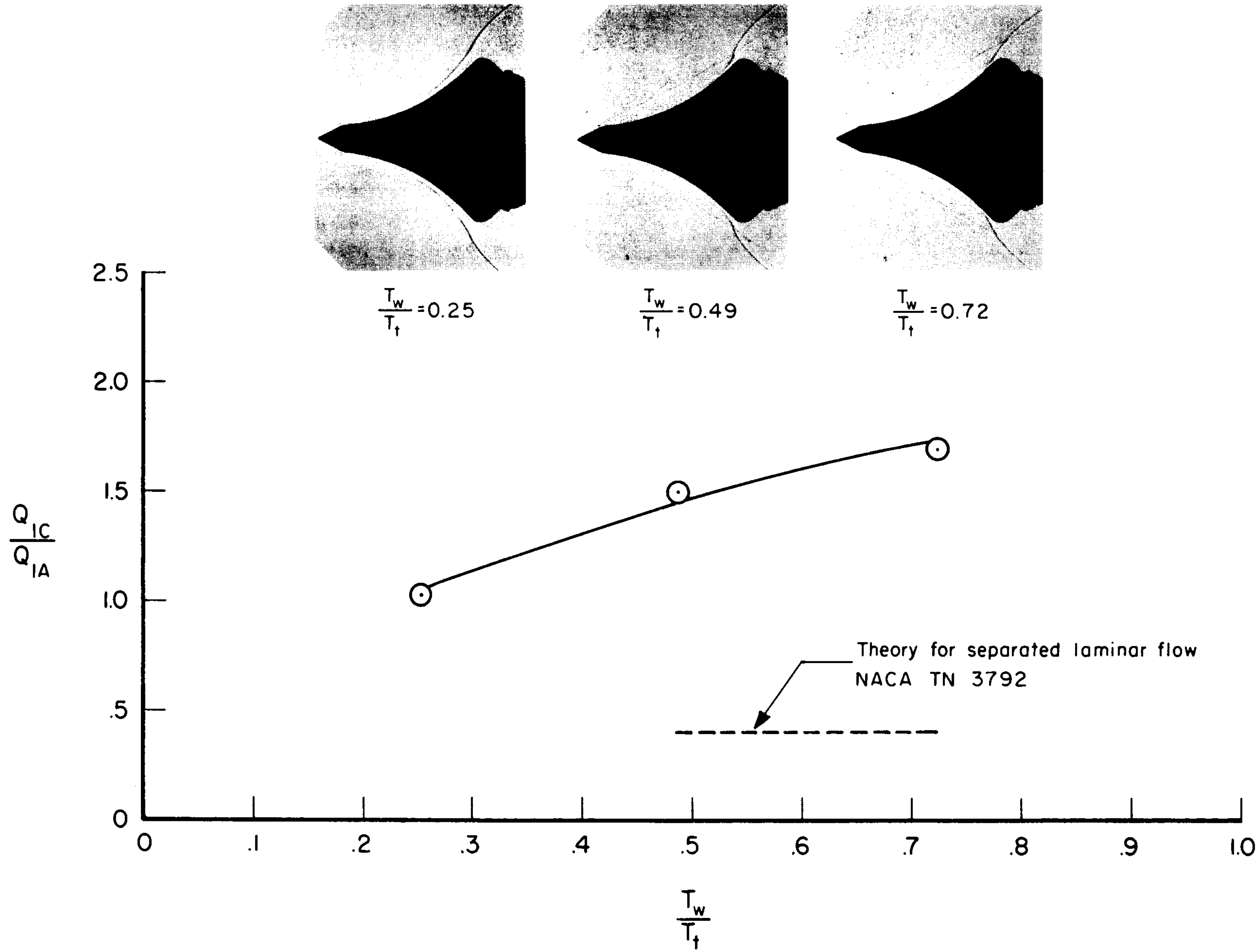

Figure 9.- Total heat transfer to model 1A compared with model 1C; $M_\infty = 5.09$, $Re_\infty = 1.2 \times 10^6$, ft^{-1}.